Energy Proceedings
Vol 29, 2022
ISSN 2004-2965

Li_2CO_3-doped Dark Calcium Carbonate Pellets for Direct Solar Energy Capture and Fast Heat Storage

Changjian Yuan[1], Xianglei Liu [1*]
1 School of Energy and Power Engineering, Nanjing University of Aeronautics and Astronautics, Nanjing 210016, China

ABSTRACT

We propose new Li_2CO_3-doped dark $CaCO_3$ pellets. The solar full-spectrum absorption of the new pellets can be as high as 73.25%. After 60 cycles, the energy storage density of the new $CaCO_3$ pellets is still as high as 1671 kJ/kg, and the decay rate of the energy storage density decreased from 56.73% to 4.24% compared with pure $CaCO_3$ pellets. At the same temperature, the average decomposition rate of the new $CaCO_3$ pellets in the first cycle is 2.1 times that of the ordinary dark $CaCO_3$ pellets. Therefore, this new $CaCO_3$ pellets can simultaneously achieve the characteristics of fast heat storage, excellent cyclic stability and high solar absorptance.

Keywords: $CaCO_3$, Li_2CO_3, fast heat storage, cyclic stability, solar absorptance

1. INTRODUCTION

The large-scale use of fossil fuels has caused serious environmental pollution and energy crisis. As a renewable energy, solar energy has the advantages of abundant resources, no pollution to the environment, and wide distribution. Therefore, the use of solar energy to solve the growing energy demand and environmental problems has received more and more attention [1-3]. Concentrated solar power (CSP) system, which integrates power generation and energy storage, is a renewable energy power generation method. Thermochemical heat storage (TCHS) is an emerging technology applied in third-generation concentrated solar power plants. TCHS has many advantages such as high heat storage density, wide operating temperature range and outstanding safety [4-7]. Calcium-Looping (CaL) system has a wide range of applicability at reaction temperatures ranging from mid-high to mid-low temperature [6, 8-11]. It is one of the most promising thermochemical heat storage systems for large-scale applications. The thermochemical heat storage principle of CaL is that $CaCO_3$ decomposes CO_2 to absorb heat, and CaO absorbs CO_2 to release heat. It can be represented by the following reversible chemical formula:

$$CaCO_3(s) \leftrightarrow CaO(s) + CO_2(g) \quad \Delta H = 178 kJ/mol \quad (1)$$

The $CaCO_3$/CaO energy storage cycle system is shown in Fig 1. Sunlight is irradiated into the calciner through a field of heliostats, and the CaCO3 pellets decompose in the calciner when they absorb solar heat directly or indirectly. The products CaO and CO_2 enter the corresponding storage tanks, respectively. Subsequently, CaO and CO_2 are introduced into the carbonator as required, releasing heat through the carbonation reaction. The high-temperature and high-pressure carbon dioxide then enters a turbine to generate electricity through a closed carbon dioxide Brayton cycle.

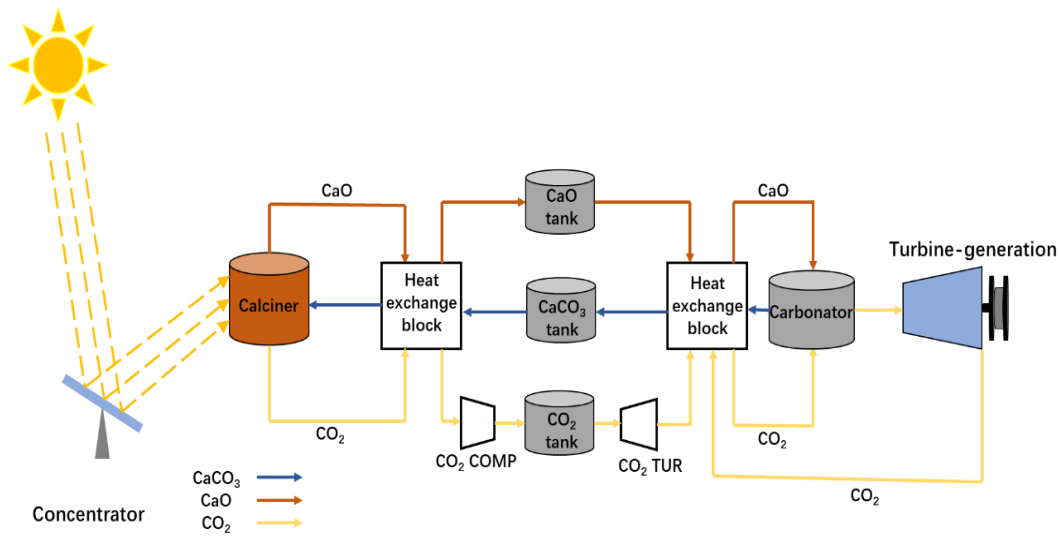

Fig. 1 The $CaCO_3$/CaO energy storage cycle system.

How to effectively capture solar radiation energy is an important issue in the $CaCO_3$/CaO energy storage cycle system. In conventional solar receivers, solar energy is usually absorbed by a surface coating and then radiated to the reactants through the surface coating [12-15]. This indirect way of absorbing solar energy has huge drawbacks, such as severe heat loss caused by coating radiation and large thermal resistance between pellets and coating. Therefore, volumetric solar technology is considered to be a more suitable technology for CaL TCHS systems. It can effectively overcome the above problems, and the solar absorption rate of the reactant is very high, so it can directly absorb a large amount of solar decompsition kinetics of $CaCO_3$[25-27]. Unlike inert dopants, the effect of alkali metal salts on the cycling stability of $CaCO_3$/CaO is complex[28-33], with often conflicting results. Han et al.[33] found that doping with alkali metal carbonates can accelerate the ion diffusion during the decomposition process, thereby increasing the decomposition rate of $CaCO_3$ and reducing the decarburization radiation energy. However, pure $CaCO_3$ pellets are white, which requires adding some dark substances to enhance their solar energy absorptivity[16-21]. It has been reported that doping Mn and Fe elements can effectively improve the solar energy absorption rate of $CaCO_3$.

In addition, the rapid decomposition of $CaCO_3$ at moderate temperatures is also of great significance. This is due to mature and inexpensive metal alloy solar receivers that only work well below 800°C [22, 23]. However, the decomposition rate of $CaCO_3$ is slow below 800 °C [24], resulting in low energy conversion efficiency. Doping of alkali metal salts is considered to be an effective way to improve the temperature. They also found that Li_2CO_3-doped dolomite still maintained good cycling stability compared to sodium carbonate and potassium carbonate. Therefore, we choose to dope Li_2CO_3 in the $CaCO_3$ pellets, which can accelerate the ion diffusion during the decomposition of $CaCO_3$ while maintaining good cyclic stability, thereby increasing the rate of thermochemical energy storage.

2. EXPERIMENTAL SECTION

2.1 Material synthesis

All chemical reagents used in this experiment are Analytical Reagent (AR). The doped pellets are prepared by the extrusion-spheronization method. The specific production process is shown in Fig. 2. Firstly, the pre calculated 50wt% $Mn(NO_3)_2$ solution (3.579g), $Fe(NO_3)_3 \cdot 9H2O$ (8.08g), $Al(NO_3)_3 \cdot 9H2O$ (11.2539g) and deionized water (20ml) are fully mixed in a beaker. Then, $Ca(OH)_2$ powder (14.818g), 80wt%(80wt% is 80% of the mass of $CaCO_3$) microcrystalline cellulose (MCC) (16g) and Li_2CO_3 powder in different molar ratios to $Ca(OH)_2$ (5%、7.5% and 10%) are fully mixed in an another beaker. The mixture solution is slowly dropped into another beaker at room temperature. Then, well-mixed samples are made into rod-shaped samples with their diameter of 0.6 mm by a screw extruder and the rod-shaped samples are added into the spheronizator to produce spherical pellets. The pellets in different sizes are prepared via the extrusion-spheronization method. Pellets can be further screened as needed. Subsequently, the spherical pellets are calcined at 700℃ for 3 h. Finally, dark samples are carbonated in a tube furnace with the reaction atmosphere (100% CO_2) and a heating rate of 10℃/min at the 700℃for 5 h. The designed dark pellets doped with n% molar ratio Li_2CO_3 are named as co-doped calcium carbonate (Cn-$CaCO_3$). The designed white pellets doped only with Al^{3+} are named as aluminum-doped calcium carbonate (A-$CaCO_3$). The designed dark pellets doped without Li_2CO_3 are named doped calcium carbonate (D-$CaCO_3$). $CaCO_3$ without Mn^{2+}, Al^{3+}, Fe^{3+} and Li_2CO_3 doping is prepared using a similar procedure and named pure calcium carbonate (P-$CaCO_3$). Unless otherwise specified, the amount of MCC added to all samples is 80%wt by default.

Table 1. Names and element molar ratios corresponding to different samples.

Name	Molar ratio
P-$CaCO_3$	Ca
A-$CaCO_3$	Ca:Al=100:15
D-$CaCO_3$	Ca:Al:Mn:Fe=100:15:5:10
C5-$CaCO_3$	Ca:Al:Mn:Fe:Li_2CO_3=100:15:5:10:5
C7.5-$CaCO_3$	Ca:Al:Mn:Fe:Li_2CO_3=100:15:5:10:7.5
C10-$CaCO_3$	Ca:Al:Mn:Fe:Li_2CO_3=100:15:5:10:10
C40-$CaCO_3$	Ca:Al:Mn:Fe:Li_2CO_3=100:15:5:10:40

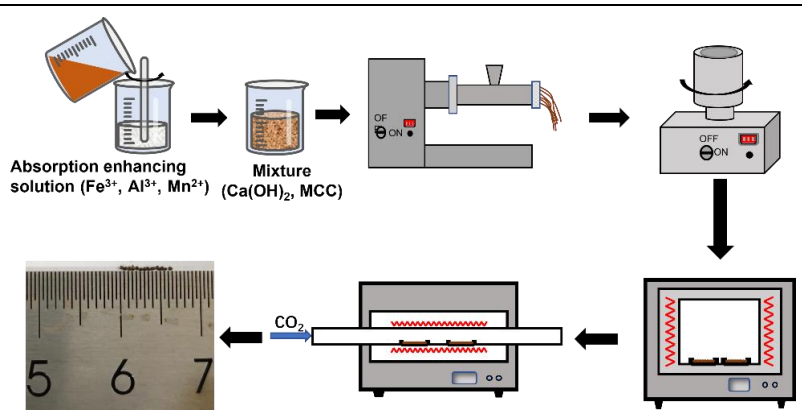

Fig. 2 Schematic preparation process of $CaCO_3$ pellets.

2.2 Instrumentations and methods

2.2.1 The average solar absorptance

The spectral reflectance R(λ) of the samples as a function of wavelength λ is measured by a UV-Vis spectrophotometer

(Lambda 1050+, PerkinElmer Inc., USA). The pellets are ground into powder in a mortar, loaded into the sample chamber and compacted for measurement. The spectral absorbance can be obtained from the formula: A(λ) = 100% - R(λ). In the 280-2000 nm band, the average solar absorptivity of the powder can be expressed by the following weighted integral formula as

$$A = \frac{\int_{280}^{2000} A(\lambda) I(\lambda) d\lambda}{\int_{280}^{2000} I(\lambda) d\lambda} \quad (2)$$

where I(λ) is the AM1.5 spectral irradiance of the sun reaching the earth's surface.

2.2.2 Thermochemical heat storage performance

The cycle performance of the fabricated pellets is measured using a thermogravimetric (TG) analytical device (STD 650, TA Instrument). The particle size range of all samples is 300-500 μm, and the added sample mass is up to 6 mg. The temperature of the carbonation process is set to 725°C. The atmosphere during carbonation is set to 50% CO_2 and 50% N2, and the carbonation time is 20 minutes. To simplify the cycle process and reduce the decomposition temperature, the M_{CO_2} is molar mass of CO_2. ΔH is the reaction molar enthalpy of the carbonation reaction (178 kJ/mol).

3. RESULTS AND DISCUSSION

3.1 XRD analysis

The XRD spectra of different $CaCO_3$ pellets are shown in Fig. 3. It can be seen that the main peaks of different $CaCO_3$ pellets are roughly the same, and they are basically the diffraction peaks of $CaCO_3$. We cannot clearly see the decomposition temperature is set to be the same as the carbonation process. The atmosphere in the decomposition process is set to pure N_2, and the decomposition time is 15 minutes.

By measuring the ability of $CaCO_3$ sample to decompose CO_2 per unit mass (D_n, g CO_2/g calcium carbonate pellets, g/g), and the CO_2 absorption capacity of calcined sample per unit mass (C_n, g CO_2/g calcined sample, g/g), weight decomposition rate (R_n, g CO_2/g calcium carbonate sample/min, $g.g^{-1}.min^{-1}$). D_n, C_n, R_n are calculated using the Eqs. (3-5), respectively.

$$D_n = \frac{m_{car,n} - m_{cal,n}}{m_{car,n}} \quad (3)$$

$$C_n = \frac{m_{car,n} - m_{cal,n}}{m_{cal,n}} \quad (4)$$

$$R_n = \frac{dD_n^t}{dt} \quad (5)$$

where $m_{Carb,n}$ and $m_{Cal,n}$ are samples' mass after and before carbonation over n cycles, respectively. The energy storage density E_n, which represents the actual energy stored per unit mass CaO, is expressed as

$$E_n = \frac{m_{car,n} - m_{cal,n}}{m_{cal,n}} \cdot \Delta H / M_{CO_2} \quad (6)$$

diffraction peaks of Li_2CO_3 from C10-$CaCO_3$, because many of the diffraction peaks of Li_2CO_3 coincide with those of $CaCO_3$. Therefore, we prepared C40-$CaCO_3$ by extrusion-spheronization method and detected its XRD spectrum. From this, the diffraction peaks of Li_2CO_3 can be clearly seen, and there are no diffraction peaks different from those of the previous samples. Therefore, it can be determined that the doped Li_2CO_3 does not produce new substances.

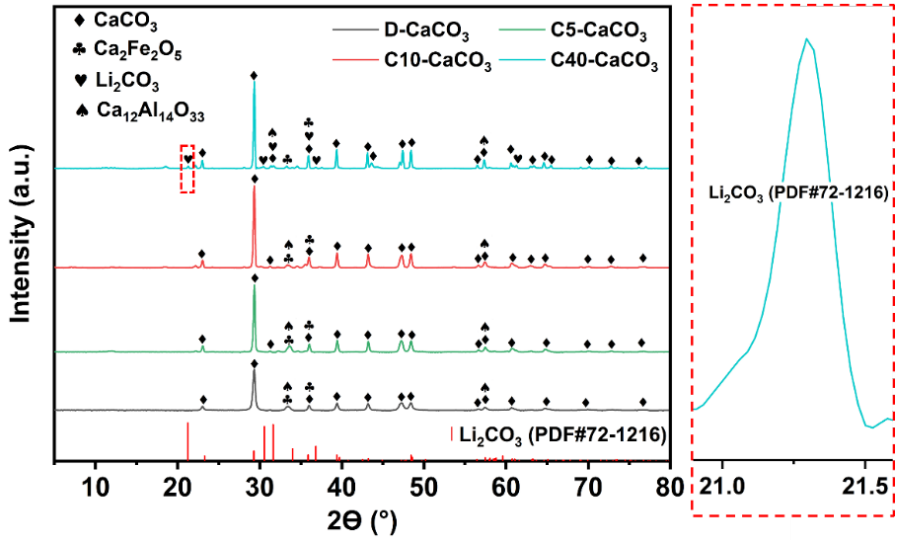

Fig. 3 XRD spectra of different $CaCO_3$ pellets

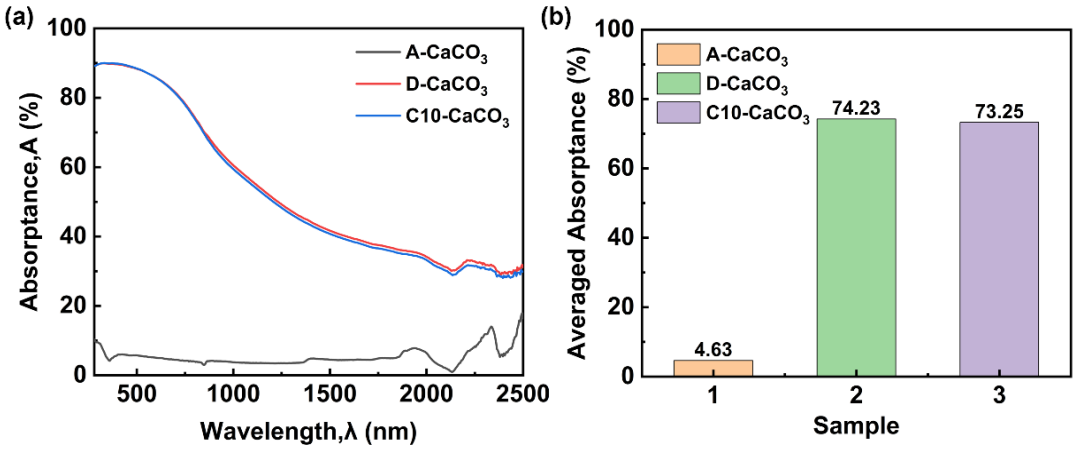

Fig. 4 (a) Absorption spectra of different samples, (b) Average solar absorptance for different samples.

3.2 Solar absorptance

It can be seen from Fig. 4(a) that the absorption rate of D-$CaCO_3$ is enhanced in almost the entire solar spectrum, where the ability of A-$CaCO_3$ to capture solar energy is very weak. As a can be seen from Fig. 4(b), the average solar absorptivity difference between C10-$CaCO_3$ and D-$CaCO_3$ is about 1%, indicating that doping lithium carbonate has little effect on the spectral absorption rate. Obviously, we can see that by doping with Mn and Fe elements and Li_2CO_3, the average solar absorptivity of $CaCO_3$ pellets is significantly increased from 4.63% to 73.25% by about 1580%. This makes it possible to directly irradiate calcium-based pellets for rapid solar thermochemical heat storage.

3.3 Thermogravimetric analysis results

The cyclic stability of different samples is shown in Fig. 5. Since A-$CaCO_3$ could not be completely decomposed in 15 minutes, the decomposition time of A-$CaCO_3$ is increased

to 25 minutes, and the CO_2 adsorption time is extended to 30 minutes. During the decomposition of $CaCO_3$, when the weight of the sample remains basically unchanged, the decomposition process is deemed to be over. The cycle performance of P-$CaCO_3$ pellets prepared by extrusion-spheronization method is significantly reduced by 36.73% after 12 cycles. However, the performance of new C10-$CaCO_3$ pellets decreased by only 4.14% after 12 cycles，which is even slightly lower than the 4.38% of D-$CaCO_3$ without Li_2CO_3 addition. The weight and energy storage density changes of P-$CaCO_3$ and C10-$CaCO_3$ after 60 cycles are shown in Fig. 6. The cycling performance of P-CaCO3 pellets decreased significantly by 56.73% after 60 cycles. However, the performance of the new C10-$CaCO_3$ pellets only dropped by 4.26% after 60 cycles. At the 12th cycle, the energy storage density of C10-$CaCO_3$ started to be higher than that of P-$CaCO_3$, and the energy storage density of C10-$CaCO_3$ is still as high as 1671 kJ/kg after 60 cycles.

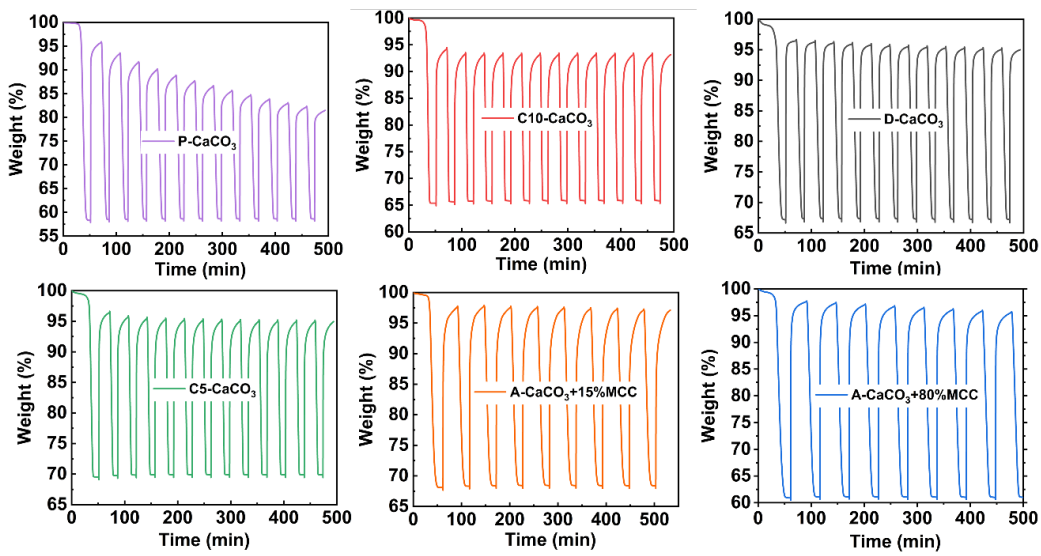

Fig. 5 Cyclic stability of different calcium carbonate samples.

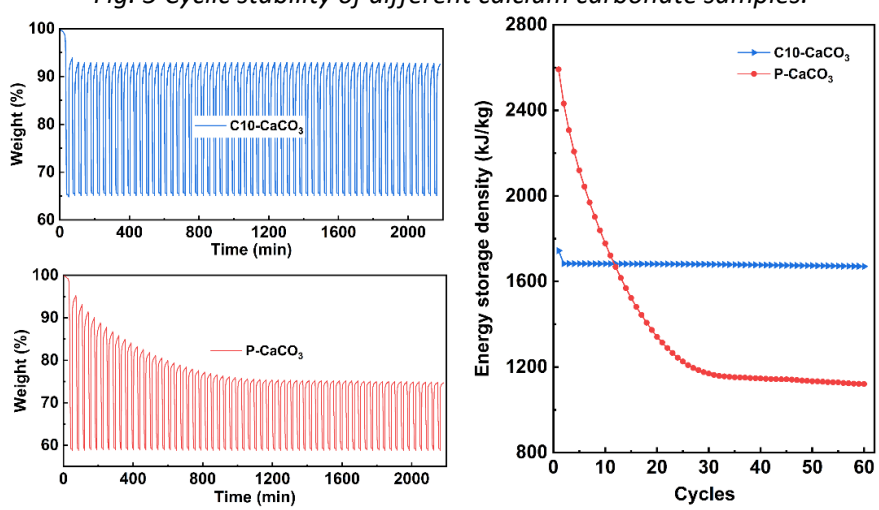

Fig. 6 Changes in weight and energy storage density of P-$CaCO_3$ and C10-$CaCO_3$ over 60 cycles

3.4 $CaCO_3$ decomposition rate

Decomposition rate and CO_2 adsorption capacity of different samples are shown in Fig. 7. It can be seen that the addition of Mn and Fe elements and a large amount of MCC can play a certain role, and Li_2CO_3 has a particularly obvious role in promoting the decomposition rate of $CaCO_3$. Comparing (a) and (b) in Fig. 7, it can be found that the decomposition rate of $CaCO_3$ spheres doped with lithium carbonate decreased significantly after 12 cycles, and the decomposition rate of other $CaCO_3$ pellets decreased slightly, which is not obvious. Alkali carbonates tend to separate from the bulk CaO during cycling and accumulate on the surface, from where they eventually desorb completely from the adsorbent. Therefore, the alkali metal content in the adsorbent decreases with cycling. However, in Fig 7. (c), it is found that with the increase of the cycle, the decrease of the reaction rate becomes lower and lower. The decomposition rate of C10-$CaCO_3$ is still slightly higher than that of C7.5-$CaCO_3$ in the first cycle after 60 cycles, and significantly higher than that of P-$CaCO_3$ and D-$CaCO_3$. Therefore, this shows that the fast decomposition rate of C10-$CaCO_3$ has an excellent advantage in long cycles. The average decomposition rate of C10-$CaCO_3$ in the first cycle is 2.1 times that of the D-$CaCO_3$ pellets and 1.85 times that of the P-$CaCO_3$ pellets. With the increase of cycle times, the decomposition rate of C10-$CaCO_3$ pellets decreased, but the decreasing range is smaller and smaller. After 60 cycles, the decomposition rate of the C10-$CaCO_3$ is still 1.82 times that of P-$CaCO_3$ pellets. In industrial applications, the decomposition rate of $CaCO_3$ pellets can be kept at the maximum value by continuously adding $CaCO_3$ pellets, so as to achieve efficient energy conversion. Therefore, the peak decomposition rate of $CaCO_3$ pellets is very important. The peak decomposition rate of the C10-$CaCO_3$ pellets in the first cycle is 2.23 times that of the D-$CaCO_3$ pellets and 1.85 times that of the P-$CaCO_3$ pellets. The 12th cycle peak decomposition rate of C10-$CaCO_3$ is 2 times that of D-$CaCO_3$ pellets.

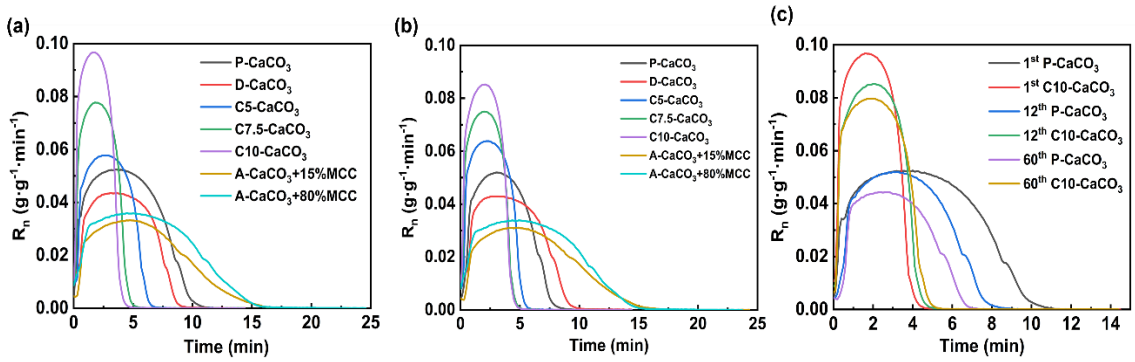

Fig. 7 Decomposition rate and CO_2 adsorption capacity of different samples: (a) The first cycle $CaCO_3$ decomposition rate (b) Twelfth cycle $CaCO_3$ decomposition rate (c) Decomposition rate of P-$CaCO_3$ and C10-$CaCO_3$ under different cycles

4. CONCLUTION

This work is devoted to the synthesis of dark calcium carbonate pellets for direct solar energy absorption and fast and efficient heat storage. The $CaCO_3$ pellets, doped with Li_2CO_3, a large amount of MCC, and elements of Al, Mn, and Fe, can be used for direct solar energy absorption in TCES systems. The full-spectrum solar absorption rate of this pellets can be as high as 73.25%, which is 1580% higher than that of $CaCO_3$ doped with Al element. It is worth noting that doping Li_2CO_3 has little effect on the solar absorptance of the material. After 60 cycles, the energy storage density of new $CaCO_3$ pellets is still as high as 1671 kJ/kg, and the decay rate of the energy storage density decreased from 56.73% to 4.24% compared with pure $CaCO_3$ pellets. At the same temperature, the average decomposition rate of new $CaCO_3$ pellets in the first cycle is 2.1 times that of the ordinary dark $CaCO_3$ pellets, and the peak decomposition rate is 2.23 times that of the ordinary dark $CaCO_3$ pellets. As the number of cycles increased, the decomposition rate of the new $CaCO_3$ pellets decreased, but the decline in decomposition rate is less and less. Even the decomposition rate of the new $CaCO_3$ pellets of the 60th cycle is 1.84 times that of the ordinary dark $CaCO_3$ pellets of the first cycle. Therefore, this new $CaCO_3$ pellets can simultaneously achieve the characteristics of fast heat storage, excellent cyclic stability and high solar absorptance. This work paves the way for the direct capture of solar energy and fast heat storage during CaL process at moderate temperature, with great prospects for industrial applications.

ACKNOWLEDGEMENT

This work is supported by the National Natural Science Foundation of China (No. 51820105010).

REFERENCE

[1] Ahmed FE, Hashaikeh R, Hilal N. Solar powered desalination – Technology, energy and future outlook. Desalination. 2019;453:54-76.

[2] Leonard MD, Michaelides EE, Michaelides DN. Energy storage needs for the substitution of fossil fuel power plants with renewables. Renewable Energy. 2020;145:951-62.

[3] Rabaia MKH, Abdelkareem MA, Sayed ET, Elsaid K, Chae KJ, Wilberforce T, et al. Environmental impacts of solar energy systems: A review. Sci Total Environ. 2021;754:141989.

[4] Alva G, Lin Y, Fang G. An overview of thermal energy storage systems. Energy. 2018;144:341-78.

[5] Dunstan MT, Donat F, Bork AH, Grey CP, Muller CR. CO2 Capture at Medium to High Temperature Using Solid Oxide-Based Sorbents: Fundamental Aspects, Mechanistic Insights, and Recent Advances. Chem Rev. 2021;121:12681-745.

[6] Gkaroutsou M, Tsampasis E, Elias C, Stathopoulos V. Thermochemical Energy Storage in Solar Power Plants. 2021 10th Mediterranean Conference on Embedded Computing (MECO)2021. p. 1-4.

[7] Mofijur M, Mahlia T, Silitonga A, Ong H, Silakhori M, Hasan M, et al. Phase Change Materials (PCM) for Solar Energy Usages and Storage: An Overview. Energies. 2019;12.

[8] Bayon A, Bader R, Jafarian M, Fedunik-Hofman L, Sun Y, Hinkley J, et al. Techno-

economic assessment of solid–gas thermochemical energy storage systems for solar thermal power applications. Energy. 2018;149:473-84.
[9] Liu D, Xin-Feng L, Bo L, Si-quan Z, Yan X. Progress in thermochemical energy storage for concentrated solar power: A review. International Journal of Energy Research. 2018;42:4546-61.
[10] Ortiz C, Valverde JM, Chacartegui R, Perez-Maqueda LA, Giménez P. The Calcium-Looping (CaCO3/CaO) process for thermochemical energy storage in Concentrating Solar Power plants. Renewable and Sustainable Energy Reviews. 2019;113.
[11] Prieto C, Cooper P, Fernández AI, Cabeza LF. Review of technology: Thermochemical energy storage for concentrated solar power plants. Renewable and Sustainable Energy Reviews. 2016;60:909-29.
[12] Bello M, Subramani S, Bin Mohd Rashid MM. The impact of Fe3O4 on the performance of ultrathin Ti/AlN/Ti tandem coating on stainless-steel for solar selective absorber application. Results in Physics. 2020;19.
[13] Caron S, Garrido J, Ballestrín J, Sutter F, Röger M, Manzano-Agugliaro F. A comparative analysis of opto-thermal figures of merit for high temperature solar thermal absorber coatings. Renewable and Sustainable Energy Reviews. 2022;154.
[14] Noč L, Šest E, Kapun G, Ruiz-Zepeda F, Binyamin Y, Merzel F, et al. High-solar-absorptance CSP coating characterization and reliability testing with isothermal and cyclic loads for service-life prediction. Energy & Environmental Science. 2019;12:1679-94.
[15] Reoyo-Prats R, Carling Plaza A, Faugeroux O, Claudet B, Soum-Glaude A, Hildebrandt C, et al. Accelerated aging of absorber coatings for CSP receivers under real high solar flux – Evolution of their optical properties. Solar Energy Materials and Solar Cells. 2019;193:92-100.
[16] Al-Shankiti IA, Ehrhart BD, Ward BJ, Bayon A, Wallace MA, Bader R, et al. Particle design and oxidation kinetics of iron-manganese oxide redox materials for thermochemical energy storage. Solar Energy. 2019;183:17-29.
[17] Aftab W, Shi J, Qin M, Liang Z, Xiong F, Usman A, et al. Molecularly elongated phase change materials for mid-temperature solar-thermal energy storage and electric conversion. Energy Storage Materials. 2022;52:284-90.
[18] Li B, Li Y, Dou Y, Wang Y, Zhao J, Wang T. SiC/Mn co-doped CaO pellets with enhanced optical and thermal properties for calcium looping thermochemical heat storage. Chem Eng J. 2021;423.
[19] Song C, Liu X, Zheng H, Bao C, Teng L, Da Y, et al. Decomposition kinetics of Al- and Fe-doped calcium carbonate particles with improved solar absorbance and cycle stability. Chem Eng J. 2021;406.
[20] Teng L, Xuan Y, Da Y, Liu X, Ding Y. Modified Ca-Looping materials for directly capturing solar energy and high-temperature storage. Energy Storage Materials. 2020;25:836-45.
[21] Zheng H, Song C, Bao C, Liu X, Xuan Y, Li Y, et al. Dark calcium carbonate particles for simultaneous full-spectrum solar thermal conversion and large-capacity thermochemical energy storage. Solar Energy Materials and Solar Cells. 2020;207.
[22] Ávila-Marín AL. Volumetric receivers in Solar Thermal Power Plants with Central Receiver System technology: A review. Solar Energy. 2011;85:891-910.

[23] Reich L, Melmoth L, Yue L, Bader R, Gresham R, Simon T, et al. A Solar Reactor Design for Research on Calcium Oxide-Based Carbon Dioxide Capture. Journal of Solar Energy Engineering. 2017;139.
[24] Zheng H, Liu X, Xuan Y, Song C, Liu D, Zhu Q, et al. Thermochemical heat storage performances of fluidized black CaCO3 pellets under direct concentrated solar irradiation. Renewable Energy. 2021;178:1353-69.
[25] Nygård HS, Tomkute V, Olsen E. Kinetics of CO2 Absorption by Calcium Looping in Molten Halide Salts. Energy Procedia. 2017;114:250-8.
[26] Tomkute V, Solheim A, Olsen E. Investigation of High-Temperature CO2 Capture by CaO in CaCl2 Molten Salt. Energy & Fuels. 2013;27:5373-9.
[27] Tomkute V, Solheim A, Olsen E. CO2 Capture by CaO in Molten CaF2–CaCl2: Optimization of the Process and Cyclability of CO2 Capture. Energy & Fuels. 2014;28:5345-53.
[28] Derevschikov VS, Lysikov AI, Okunev AG. Sorption properties of lithium carbonate doped CaO and its performance in sorption enhanced methane reforming. Chem Eng Sci. 2011;66:3030-8.
[29] Ge Z, Jiang F, Chen Q, Wang L, Ding Y, Chen H. The role of MgO supported sodium sulfate molten salt for calcium looping thermochemical energy storage. Chem Eng J. 2022;444.
[30] Huang L, Zhang Y, Gao W, Harada T, Qin Q, Zheng Q, et al. Alkali Carbonate Molten Salt Coated Calcium Oxide with Highly Improved Carbon Dioxide Capture Capacity. Energy Technology. 2017;5:1328-36.
[31] Lee CH, Choi SW, Yoon HJ, Kwon HJ, Lee HC, Jeon SG, et al. Na2CO3-doped CaO-based high-temperature CO2 sorbent and its sorption kinetics. Chem Eng J. 2018;352:103-9.
[32] Salvador C, Lu D, Anthony EJ, Abanades JC. Enhancement of CaO for CO2 capture in an FBC environment. Chem Eng J. 2003;96:187-95.
[33] Han R, Xing S, Wu X, Pang C, Lu S, Su Y, et al. Relevant influence of alkali carbonate doping on the thermochemical energy storage of Ca-based natural minerals during CaO/CaCO3 cycles. Renewable Energy. 2022;181:267-77.